



# Conceptual design of a pilot assistance system for customised noise abatement departure procedures

Joscha Kurz<sup>1</sup> · Jason Blinstrub<sup>2</sup>

Received: 17 February 2023 / Revised: 30 October 2023 / Accepted: 31 October 2023  
© The Author(s) 2023

## Abstract

The departure of an aircraft is commonly the flight phase with the highest thrust level in a flight, which leads to considerable noise levels on the ground. The departure procedures are characterised by the thrust reduction altitude, the acceleration altitude, and the control of airspeed and aircraft configuration within each take-off segment. Thrust reduction and acceleration altitudes are typically constant and are not adjusted to particular operational key parameters (e.g., take-off mass, reduced take-off thrust) or weather conditions. However, the parameters differ between individual flights and affect flight performance as well as the noise levels on the ground. This paper presents the conceptual design of a pilot assistance system which aims to reduce the noise on the ground by identifying a custom thrust reduction and acceleration altitude for existing noise abatement departure procedures. The pilot assistance system is based on an aircraft simulation model and a noise simulation and is aimed to be utilised during pre-flight planning on ground. A key part of the noise evaluation is that the local population distribution around the airport is considered. An overview of the ongoing research at the German Aerospace Center is provided. The conceptual design and preliminary results are presented and discussed using an exemplary take-off for three wind conditions.

**Keywords** Aircraft noise · Noise abatement · Departure procedure · Take-off · Pilot assistance system · NADP

## Abbreviations

|       |  |          |  |
|-------|--|----------|--|
| AGL   | Above Ground Level   | FCU      | Flight Control Unit  |
| AIP   | Aeronautical Information Publication   | FMGC     | Flight Management and Guidance Computer                      |
| ATRA  | Advanced Technology Research Aircraft  | FMGS     | Flight Management and Guidance System                        |
| AzB   | Anleitung zur Berechnung von Lärmschutzbereichen (Guidance for the calculation of noise protected areas) | ICAO     | International Civil Aviation Organization                    |
| CAS   | Calibrated airspeed  | LNAS     | Low Noise Augmentation System                                |
| DFS   | Deutsche Flugsicherung   | MCDP     | Multi Criteria Departure Procedure                           |
| DLR   | Deutsches Zentrum für Luft- und Raumfahrt (German Aerospace Center)                                      | MCDU     | Multipurpose Control and Display Unit                        |
| ECAC  | European Civil Aviation Conference   | NADP     | Noise Abatement Departure Procedure                          |
| EFB   | Electronic Flight Bag  | NIROS    | Noise Impact Reduction and Optimization System               |
| FADEC | Full Authority Digital Engine Control  | PANS-OPS | Procedures for Air Navigation Services - Aircraft Operations |
|       |  | PEP      | Performance Engineer's Program                               |
|       |  | SID      | Standard Instrument Departure                                |
|       |  | TOGA     | Take-off/Go-around   |
|       |  | V1       | Decision speed   |
|       |  | V2       | Take-off safety speed  |
|       |  | VR       | Rotation speed   |
|       |  | Vzf      | Zero flaps speed   |
|       |  | WGS84    | World Geodetic System 1984                                   |
|       |  | WHO      | World Health Organization                                    |

✉ Joscha Kurz  
joscha.kurz@dlr.de  
Jason Blinstrub  
jason.blinstrub@dlr.de

<sup>1</sup> Institute of Flight Systems, German Aerospace Center (DLR), Lilienthalplatz 7, 38108 Braunschweig, Germany

<sup>2</sup> Institute of Aerodynamics and Flow Technology, German Aerospace Center (DLR), Bunsenstr. 10, 37073 Göttingen, Germany

## 1 Introduction

The European Aviation Environmental Report 2022 expects that the total number of arriving and departing flights is going to grow to 12.2 million in 2050 for the most likely future scenario by using airports of the 27 member states of the European Union and the European Free Trade Association, compared to 9.25 million in 2019 [1]. Increasing public awareness of global climate change and the health effects of noise indicate that ecological aspects and aircraft noise become more meaningful besides economic efficiency. The European Aviation Environmental Report specifies that the exposure to aircraft noise affects the health and wellbeing as for example in the form of stress caused by the annoyance, sleep disturbance, heart disease, premature mortality due to ischemic heart disease, and learning impairment to children [1]. Furthermore, it has been shown that residents feel more annoyed by aircraft noise than that caused by other transport sources [2]. The World Health Organization (WHO) recommended in 2018 to implement measures to reduce the day-evening-night noise level below 45 dB, as higher levels are associated with adverse health effects. During night time the WHO recommended to reduce noise exposure below 40 dB, as higher levels are associated with adverse effects on sleep [3]. The objectives of the European Commission's *Flightpath 2050* agreement are to reduce CO<sub>2</sub> emissions per passenger kilometre by 75 %, NO<sub>x</sub> emissions by 90 %, and perceived noise by 65 % by 2050 compared to the capabilities of a typical new aircraft in 2000 [4]. The Balanced Approach of the International Civil Aviation Organization (ICAO) encompasses four principle elements to address aircraft noise problems where they occur, for an individual airport-by-airport approach: reduction of noise at source, land-use planning and management, noise abatement operational procedures, and operating restrictions on aircraft [5]. Noise abatement operational procedures, such as noise preferential routes, standard instrument departures (SID), standard terminal arrival routes, dispersed flight tracks, automated procedures, noise preferential runways, displaced thresholds, or noise abatement departure and approach procedures [5], have the notable advantage that aircraft with an aged technical level are able to apply those measures. This is beneficial, because those aircraft are still in service and usually emit more noise at the source compared to new aircraft. Furthermore, operational measures have the benefit that they can provide short- to mid-term solutions for reducing the noise exposure at certain locations. On the other side, the development and implementation of new aircraft or low-noise technology modifications (e.g., fairings, acoustic liners, low-noise fan, chevron nozzle) generally require more

time. In general, noise abatement departure procedures can be used to optimise the noise and its distribution on the ground by modifying procedural pilot inputs and their timing along the flight path. Typical inputs are for example the aircraft configuration, the engine thrust level, or the speed that affect the altitude and thus also noise. Established procedures could be optimised and flown more precisely with the help of new appropriate assistance systems.

### 1.1 State of technology

The noise levels on ground during take-off are mainly affected by the flight condition (e.g., aircraft mass, thrust level, aircraft configuration), the departure procedure, the routing, the weather, and instructions by the air traffic control. During take-off, the noise levels on ground are dominated by engine sound sources, whereas aerodynamic sound sources can be neglected [6].

Aircraft departure procedures are typically defined by the operator, i.e., the airline. Commission Regulation (EC) No. 859/2008 specifies that an operator shall establish appropriate departure procedures for each aircraft type. The operator shall ensure that safety has priority over noise abatement. The operator also has to ensure that these procedures are designed to be simple and safe to operate with no significant increase in crew workload during critical phases of flight. Two departure procedures shall be defined for each aeroplane type, in accordance with ICAO Doc. 8168 (Procedures for Air Navigation Services - Aircraft Operations, *PANS-OPS*), Volume I:

1. noise abatement departure procedure one (NADP-1), designed to meet the close-in noise abatement objective; and
2. noise abatement departure procedure two (NADP-2), designed to meet the distant noise abatement objective; and
3. in addition, each NADP climb profile can only have one sequence of actions [7].

The *PANS-OPS* describe, among others, recommended operational procedures and are intended for the guidance of procedures specialists. The *PANS-OPS* provide two examples for departure procedures to reduce exposure to noise on ground. One of the main differences between NADP-1 and NADP-2 is that the acceleration segment for flap/slat retraction is either initiated prior to reaching the maximum prescribed height or at the maximum prescribed height. Other differences are the thrust reduction height and the speed management below the maximum prescribed height [8]. These noise abatement departure procedures are discussed in detail in Sect. 2.5. The formerly recommended and more detailed procedures ICAO-A and ICAO-B, which were

defined in a previous PANS-OPS version, were replaced in November 2001 [9].

Standard instrument departures are published in the Aeronautical Information Publication (AIP) which comprise the lateral routing, restrictions, and performance requirements (e.g., climb with 3.6 % or more until passing 4000 ft) for the departure at German airports. The AIP can also include procedural noise abatement guidelines.

In order to address air traffic noise, several tools and systems have been implemented in flight operation and for noise assessment. The Quiet Climb System by Boeing assists pilots with flying low-noise departures by the use of automatic thrust reduction and restoration along the flight path for the purpose of noise abatement. The system reduces the thrust automatically at the selected thrust reduction altitude to maintain the optimum climb angle and airspeed and restores the thrust level automatically back to full climb thrust at the selected restoration height.<sup>1</sup> The Noise Impact Reduction and Optimization System (NIROS) of Deutsche Flugsicherung (DFS) is used to evaluate routings within the planning process. It is based on a model for the prediction of noise impact on the population for a flight trajectory. Noise levels are multiplied with the population density and evaluation criteria are then calculated and used for the comparison of different routings.<sup>2</sup> For approach procedures, the German Aerospace Center (DLR) has developed the assistance system LNAS (Low Noise Augmentation System). The system visualises procedural recommendations to the pilots on the Electronic Flight Bag (EFB) by using an energy-based vertical situation display. It indicates the optimal points in time to execute actions like the setting of speeds, flaps, landing gear, and, if necessary, speed brakes. Based on live flight data, a continuous correction is carried out to provide the energy-optimal profile at any time. It helps pilots to fly low-noise and more efficient approaches [10]. For departure, Airbus and Thales have done research on the Multi Criteria Departure Procedure (MCDP) which concept is based on specific procedures by ICAO. Its intended function is to optimise noise reduction around the airport and also CO<sub>2</sub> emissions under certain mission conditions (e.g., runway, take-off mass, weather) [11, 12].

## 1.2 Problem definition

As the pilot assistance system LNAS has been developed successfully for approach procedures at DLR, a similar

system function for departure procedures is the next pace. However, in terms of the interaction between aircraft performance and noise impact on ground there is a difference for approach and departure. During approach, there is a complex interaction between height, speed, thrust, and flap setting, because engine and airframe noise are both relevant. As a result, the overall noise on the ground can be reduced by optimising this interaction. During departure, however, the only relevant noise source is the engine. Since only height and thrust can be modified, the overall noise on the ground is mostly redistributed and not reduced. This is one decisive reason why operators shall define one procedure designed to meet the close-in noise objective, and one procedure designed to meet the distant noise abatement objective [7]. The energy-optimisation of the present LNAS function enables to reduce noise during the approach. For example, approaching with idle thrust is fuel friendly, allows steep descent angles which increases the propagation distance to the ground, and reduces engine noise emissions. Furthermore, a too early extension of the high-lift devices and a preventable deployment of speed brakes can be avoided which is advantageous for fuel consumption and aerodynamic noise. In other words, the energy-optimisation effects are mostly simultaneously noise-friendly. That is different for take-off and departure. For example, applying a high thrust level increases engine noise emissions but allows steep climb angles at the same time which increases the propagation distance to the ground. Maintaining the initial climb speed and delaying the acceleration phase also allows steep climb angles, but increases fuel consumption. It can be summarised that an energy-optimised departure would result in an optimised climb performance which simply means an early acceleration phase to reach the clean configuration, the best climb speed, and a late thrust reduction. This energy-optimum is not simultaneously noise-friendly and can not meet the close-in and the distant noise abatement objective. Furthermore, the affected population distribution changes for every airport, runway, and SID. Besides that, the aircraft and weather conditions (e.g., take-off mass, take-off thrust, wind speed and direction) vary from flight to flight, which also affect the individual noise level distribution on ground. Taking into account all these factors involved for optimised departure procedures deduces to come off from general optimised noise abatement departure procedures to a customised solution for a single flight. Besides a flight simulation, such a system should include noise calculations, population data, as well as all the individual relevant boundary conditions that influence the flight trajectory. The customisation of established noise abatement departure procedures (e.g., NADP-1, NADP-2) is preferred over the introduction of new procedural steps or changes in sequence, because the implementation and application of customised procedures

<sup>1</sup> Jerry Friedrich, Daniel McGregor, Douglas Weigold. Quiet Climb. URL: [https://www.boeing.com/commercial/aeromagazine/aero\\_21/quietclimb\\_story.html](https://www.boeing.com/commercial/aeromagazine/aero_21/quietclimb_story.html) (Accessed 01.02.2023)

<sup>2</sup> Berlin Südwest gegen Fluglärm. Deutsche Flugsicherung (DFS) & Flugrouten. URL: <http://berlin-gegen-fluglaerm.de/deutsche-flugsicherung-dfs-flugrouten/> (Accessed 01.02.2023)

**Fig. 1** Screenshot of the take-off parameter determination on the EFB



is then expected to be easier and realisable within a shorter period of time.

## 2 Conceptual design

This paper proposes a concept of a pilot assistance system for the customisation of departure procedures for single flights in flight operation. The concept comprises a customisation algorithm, an aircraft trajectory simulation, a noise simulation, and population data, which are independent modules that are assembled and connected according to the function of the system. The system is focusing on the adjustment of established noise abatement departure procedures to avoid new procedural steps or changes in sequence. It is intended to be used by the pilots only during pre-flight planning and not in the air. Pilots should simply put the parameters customised by the proposed system into the Multipurpose Control and Display Unit (MCDU) or the Flight Control Unit (FCU) (Airbus A320) in order that the take-off itself can be operated as usual using managed or selected guidance.

First, the pilot determines the take-off parameters for the upcoming flight with the EFB. The operational speeds and possible thrust reduction options are calculated considering operational and performance limitations (e.g., take-off distance available, accelerate stop distance available, climb performance, obstacles) for the individual take-off. The user interface of the EFB application is shown in Fig. 1.

The fields of the airport and the runway on the screenshot are blanked for anonymity reasons. On the left side of the display are the parameters which are entered and selected by the pilot. On the right side are the calculated results including the take-off thrust options and the operational speeds. These speeds are the decision speed (V1), the rotation speed (VR), and the take-off safety speed (V2). The thrust options are take-off/go-around thrust (TOGA) and reduced take-off thrust expressed as flex temperature (e.g., F 50). The take-off parameters (e.g., aircraft mass, take-off flap setting, take-off thrust level, VR, V2) are then entered into the input page of the proposed system. These parameters are used for the customisation of the departure procedures.

### 2.1 Graphical user interface

The intention of the system is to interact with the pilot via a graphical user interface on the EFB. Figure 2 illustrates a sketch for the input page. Take-off parameters and a final climb speed are entered. Additionally, a lateral flight plan (i.e., from the SID) and a customisation mode (*NADP-Mode*) are selected. This mode allows the pilot to select which procedures are to be considered in the assessment (e.g., NADP-1 and/or NADP-2). In the future, an automatic transfer from the take-off parameter determination might be more practicable within flight operation.

Figure 3 illustrates an exemplary sketch for the output page. This page is intended to list all departure procedure options with the differences in noise, fuel, and time


| LNAS Departure  |               |              |        |        |
|---|---------------|--------------|--------|--------|
| <b>Airport</b>  | EDDX ▾        | <b>TOM</b>   | 75500  | kg     |
| <b>RWY</b>  | 08 ▾          | <b>CG</b>    | 25     | % MAC  |
|   | Full Length ▾ | <b>Wind</b>  | 0 / 0  | kt / ° |
| <b>SID</b>  | X0X1X2 ▾      | <b>OAT</b>   | 15     | °C     |
| <b>NADP-Mode</b>  | All ▾         | <b>QNH</b>   | 1013   | hPa    |
|  |               | <b>CONF</b>  | 2 ▾    | -      |
|   |               | <b>AC</b>    | Norm ▾ |        |
|   |               | <b>A-ICE</b> | Off ▾  |        |
|   |               | <b>VR</b>    | 141    | kt     |
|   |               | <b>V2</b>    | 145    | kt     |
|   |               | <b>FLX</b>   | Off ▾  | °C     |
|   |               | <b>V-CLB</b> | 250    | kt     |

Fig. 2 Sketch for the input page of the system

compared to a chosen reference procedure. The pilot can then accordingly sort and select by these evaluation parameters. The option highlighted in green predicts the most noise friendly option as the options are sorted by the noise difference in this sketch. A click on one of the procedures can open a window with further details. The  $\Delta$ Noise values are given here in percent to the selected reference procedure because the noise assessment criteria (e.g., number of awakenings) is intended to remain flexible. The noise unit is not expected to be relevant for the pilots. For this reason,

qualitative indicators are also conceivable. The number of displayed options is flexible and can be customised. It is also possible only to provide one recommendation which is based on operator policies in order to consider a trade-off between noise reduction, fuel consumption, and time. The determination of the evaluation criteria is basically part of Sect. 2.6.

### 2.2 Aircraft model

For the simulation of the departure procedures a flight dynamic model with six degrees of freedom for an Airbus A320–232 is used which is developed in MATLAB/Simulink at the German Aerospace Center. This model is based on Airbus PEP data (Performance Engineer’s Program) and flight data which are available for the DLR aircraft ATRA (Advanced Technology Research Aircraft). Furthermore, the aircraft model facilitates controllers for the manual control, the autopilot with guidance modes, the auto thrust function and the FADEC (Full Authority Digital Engine Control). Normally, the model receives its inputs from an external and comprehensive software environment which models the Flight Management and Guidance System (FMGS). These inputs include manual inputs, setpoints, and guidance modes of the Flight Management and Guidance Computer (FMGC), and inputs for the flight control logic. The conceptual design needs an automatised departure procedure simulation. For this reason, several modifications, simplifications, and additional functions have been implemented.

Fig. 3 Sketch for the output page of the system

| LNAS Departure  |                    |           |                        |           |             |          |             |           |             |            |
|-----------------|--------------------|-----------|------------------------|-----------|-------------|----------|-------------|-----------|-------------|------------|
| Procedure       | Acceleration (AGL) |           | Thrust Reduction (AGL) |           | ΔNoise      |          | ΔFuel       |           | ΔTime       |            |
|                 |                    | ft        |                        | ft        |             | %        | kg          |           | min         |            |
| NADP-2/2 ▾      | 1500               | ft        | -                      | ft        |             |          |             |           |             |            |
| <b>NADP-2/3</b> | <b>800</b>         | <b>ft</b> | <b>800</b>             | <b>ft</b> | <b>-6.1</b> | <b>%</b> | <b>+3.7</b> | <b>kg</b> | <b>+0.3</b> | <b>min</b> |
| NADP-2/1        | 800                | ft        | -                      | ft        | -5.8        | %        | -0.2        | kg        | +0.2        | min        |
| NADP-2/3        | 1000               | ft        | 1000                   | ft        | -5.3        | %        | +6.5        | kg        | +0.3        | min        |
| NADP-2/1        | 1000               | ft        | -                      | ft        | -4.9        | %        | +2.5        | kg        | +0.2        | min        |
| NADP-2/3        | 1200               | ft        | 1200                   | ft        | -4.8        | %        | +9.3        | kg        | +0.3        | min        |
| NADP-2/2        | 800                | ft        | -                      | ft        | -4.6        | %        | -8.8        | kg        | -0.1        | min        |
| NADP-2/3        | 1400               | ft        | 1400                   | ft        | -4.0        | %        | +12.2       | kg        | +0.3        | min        |
| NADP-1          | 2400               | ft        | 1200                   | ft        | -3.8        | %        | +39.9       | kg        | +0.6        | min        |
| NADP-1          | 2600               | ft        | 1000                   | ft        | -3.8        | %        | +48.7       | kg        | +0.7        | min        |
| NADP-1          | 2600               | ft        | 1200                   | ft        | -3.8        | %        | +46.2       | kg        | +0.7        | min        |



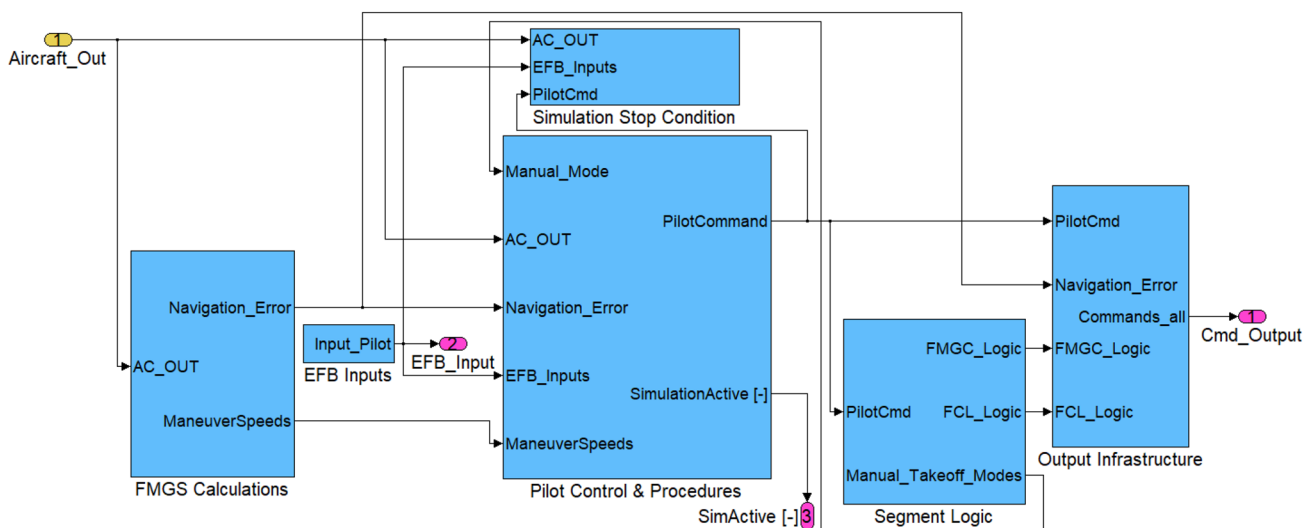


Fig. 4 Screenshot of the control structure in the aircraft model in MATLAB/Simulink

The major modification in the model is the implementation of a control structure to substitute the model inputs which are normally determined by the external software environment. This control structure (see Fig. 4) models and supplies the manual pilot inputs (e.g., sidestick, pedals, flap lever, gear lever, thrust lever) and simplified functions of the FMGS (e.g., lateral navigation, calculation of manoeuvring speeds, guidance mode switching) to simulate a departure procedure automatically. The feedback from the aircraft simulation is used as input for the control structure. The subsystem *Pilot Control and Procedures* includes the manual control, the aircraft configuration management, and the implementation of the departure procedures. The subsystem *Segment Logic* assigns flight guidance modes, flight control laws, and the newly developed manual modes for each flight segment of the procedure. For the development and the design of the control structure the Flight Crew Operating Manual (FCOM) [13–16], Aircraft Flight Manual (AFM) [17], and the Aircraft Maintenance Manual (AMM) [18] of Airbus are used. The new manual modes model the manual pilot inputs (sidestick and pedals) and control the aircraft vertically and laterally between brake release and below a height of 50 ft above ground. As there is no topography information available, this height refers to the runway threshold elevation. Then the autopilot is engaged and the speed reference system mode and navigation mode become active. The speed reference system mode remains active for the initial climb at a constant airspeed. At the acceleration altitude the climb mode is engaged for the vertical navigation. The current system has no detailed weight and balance information about the loads (i.e., fuel, payload, crew) and their positioning. For this reason, the aircraft model uses the

constant take-off mass and centre of gravity during departure which are entered by the pilot.

The wind speed and wind direction are tabularly provided as a function of the aircraft height. Historic mean wind data is used to derive a height exponent by the method of Hellmann [19] to approximate an exponential wind profile. The wind profile can then be adjusted to the real wind conditions on ground. In the future, for an appropriate accuracy in flight operation real live wind data should be used which could be transmitted by previously departed aircraft. The simplified lateral navigation allows the aircraft to follow a set of waypoints which represent the lateral flight plan. The waypoints are obtained from the AIP and are linearly connected to each other. The aircraft leaves the current segment in such a way that it intersects the next segment tangentially based on the velocity when the turn is initiated. The turn initiation is determined for a turning radius assuming a constant bank angle. The implemented vertical and lateral navigation does not consider procedure design gradients, altitude, or speed constraints. For reduced take-off thrust the model interpolates the throttle command that results in a thrust level which is equal to maximum take-off thrust for the assumed temperature (flex temperature) which is entered by the pilot. The current conceptual design model assumes dry runway conditions, normal air conditioning, and anti-ice off.

### 2.3 Noise simulation

The noise prediction is performed with the DLR research tool SIMUL. This tool has been developed to assess the noise levels on ground in more detail compared to best-practice methods like ECAC Doc 29 [20–22] or AzB [23]. The modelling of the sound is based on a separation into

partial sound sources. Currently, two engine sound components (free jet and other noise generation mechanisms of the engine) and two aerodynamic sound components (landing gear sound and sound generated by high-lift devices) are considered. For a physically correct modelling of the aircraft sound, a separate modelling of these components is crucial because those components differ significantly, especially with regard to the influence of the airspeed on the sound emission [24, 25]. Note, that the presented methodology of a conceptual design of a pilot assistance system works with other noise prediction tools as well.

## 2.4 Population data

The population distribution data around the airports are provided by the Global Human Settlement population grid of the European Commission [26]. This open and free spatial raster dataset depicts the distribution of population, mapped as the number of people per cell. The residential population is estimated for the year 2015. It is disaggregated from census or administrative units to grid cells, informed by the distribution and density of built-up areas as mapped in the Global Human Settlement Layer per corresponding epoch [27]. The data grids are available in Mollweide coordinates with a maximum resolution of 250 m or in World Geodetic System 1984 (WGS84) coordinates with a resolution of 9 arcsec.

## 2.5 Noise abatement departure procedures

The noise abatement departure procedures NADP-1 and NADP-2, as described in the PANS-OPS [8], are the basis for the customisation.

The NADP-1 includes a thrust reduction at or above the minimum initiation height of 800 ft. The initial climb speed until the initiation height shall not be less than the take-off safety speed  $V_2 + 10$  kt. After the thrust reduction a climb speed of  $V_2 + 10$  to 20 kt and the take-off configuration are maintained until an acceleration height of not more than 3000 ft. At this height the aircraft accelerates to the en-route climb speed and retracts flaps and slats on schedule.

The NADP-2 includes the initiation of acceleration and flap/slat retraction after reaching the minimum initiation height of 800 ft. The initial climb speed until the initiation height shall not be less than  $V_2 + 10$  kt. When reaching the initiation height, the aircraft accelerates towards the zero flaps speed  $V_{zf} + 10$  to 20 kt while maintaining a positive rate of climb. The flaps/slats are retracted on schedule. Thrust is reduced either with the initiation of the first flap/slat retraction or after flap/slat retraction when the clean configuration is attained. At a height of 3000 ft the aircraft accelerates to en-route climb speed.

## 2.6 Algorithm

The algorithm is written in MATLAB and is subdivided into a control structure (e.g., for inputs/outputs of models, simulation execution), the customisation, and the evaluation. The customisation is performed for the noise abatement departure procedures NADP-1 and NADP-2. It varies the combinations of the previously defined parameters (e.g., acceleration altitude, thrust reduction altitude) and the departure procedures, and presents the results to the pilot (see Fig. 3). In clear terms, the current customisation is not a real optimisation algorithm yet. The intention is just to identify an adjusted departure procedure for the single flight in order to reduce its impact on the local population in terms of noise. For NADP-2, the climb speed below 3000 ft is adjusted and three procedural modifications for thrust reduction after reaching the acceleration altitude are considered. Firstly, thrust reduction with the initiation of flap retraction (NADP-2/1). Secondly, thrust reduction when the aircraft is clean (NADP-2/2). Thirdly, thrust reduction at the beginning of the acceleration phase (NADP-2/3). The definition of the thrust reduction option of NADP-2/3 is not mentioned in the PANS-OPS but it is still implemented as it appeared as an option during literature research. For example, this departure procedure was presented as NADP-2 by Lufthansa in 2013.<sup>3</sup>

The noise impact of a single flight on the population around the airport can be assessed with arbitrary but suitable evaluation criteria. For example, the total number of expected awakenings is one possible evaluation criteria that is also used for the conceptual design. The awakening criteria describes a dose-response relationship between the maximum sound pressure level of an aircraft noise event and the probability to wake up [28]. This criteria is sensible for night-time operation and can be determined as an informative absolute value for the given population data. The awakening probability ( $P_{\text{Awake}}$ ) is calculated for each cell of the population data grid by using the AS-weighted maximum sound pressure level ( $L_{\text{AS,max}}$ ) and the second-degree polynomial [28]

$$P_{\text{Awake}} = 1.894 \cdot 10^{-3} \cdot L_{\text{AS,max}}^2 + 4.008 \cdot 10^{-2} \cdot L_{\text{AS,max}} - 3.3243. \quad (1)$$

Since this equation applies for indoor-levels only, 15 dB are subtracted from the outdoor sound pressure level to account for a partly opened window. The number of awakenings per cell is determined by multiplying the number of people per

<sup>3</sup> Markus Kreher. Takeoff Procedures: Lufthansa Passage Airline - Status April 2013, 24.04.2013. URL: [https://www.flk-frankfurt.de/eigene\\_dateien/sitzungen/220.\\_sitzung\\_am\\_24.04.2013/top\\_2\\_-\\_praes.\\_dlh\\_sachstand\\_cutback-verfahren\\_\\_24.4.2013.pdf](https://www.flk-frankfurt.de/eigene_dateien/sitzungen/220._sitzung_am_24.04.2013/top_2_-_praes._dlh_sachstand_cutback-verfahren__24.4.2013.pdf) (Accessed 01.02.2023)

**Table 1** Input parameters for the take-off examples with three different wind conditions

|                               |             |                |                |
|-------------------------------|-------------|----------------|----------------|
| Aircraft mass                 | 75.5 t      |                |                |
| Outside air temperature       | 15 °C       |                |                |
| Sea level atmosphere pressure | 1013.25 hPA |                |                |
| Centre of gravity             | 25 %        |                |                |
| Configuration                 | 2           |                |                |
| Final climb speed             | 250 kt      |                |                |
| Selected altitude             | 10,000 ft   |                |                |
| Air conditioning              | Norm        |                |                |
| Anti-ice                      | Off         |                |                |
| Full field length             | Yes         |                |                |
| Wind                          | 0 kt        | Headwind 15 kt | Tailwind 10 kt |
| Thrust                        | TOGA        | TOGA           | TOGA           |
| VR                            | 141 kt      | 141 kt         | 141 kt         |
| V2                            | 145 kt      | 145 kt         | 145 kt         |

cell ( $n_{\text{Pop},i_{\text{cell}}}$ ) with the corresponding awakening probability ( $P_{\text{Awake},i_{\text{cell}}}$ ). Finally, the total number of awakenings ( $N_{\text{Awake}}$ ) is the sum of the awakenings per cell, i.e.,

$$N_{\text{Awake}} = \sum_{i_{\text{cell}}=1}^{N_{\text{cell}}} n_{\text{Pop},i_{\text{cell}}} \cdot P_{\text{Awake},i_{\text{cell}}}, \quad (2)$$

where  $i_{\text{cell}}$  is the index for each cell and  $N_{\text{cell}}$  is the number of cells. The population within the area of the airport site is not taken into account.

The flight performance is calculated by using flight simulation results and handbook methods. The simulation for the following examples is automatically stopped when the aircraft has reached an altitude of 10,000 ft and a final climb speed of 250 kt (Note: the operational speeds in this paper are calibrated airspeeds (CAS)). Since the flight simulation ends at different distances, a distance correction is required in order to allow a fair comparison of fuel consumption and required time. This correction adds an horizontal flight segment with a length that is equal to the maximum travelled distance of all departure procedure minus the distance of each departure procedure. After the correction, all flights have the same distance travelled. Then, the differences in fuel consumption and time are calculated referring to the reference procedure. The correction is based on the in-flight performance charts for cruise from the Flight Crew Operating Manual of Airbus [15]. The fuel consumption and true airspeed of the correction are determined and estimated for the take-off mass at the optimum cruise altitude assuming international standard atmosphere conditions, a centre of gravity of 33 %, normal air conditioning, anti-icing off, and no wind.

### 3 Example

The parameters for three exemplary take-offs at a typical passenger airport are shown in Table 1. The take-off parameters which are determined with the EFB for three wind conditions are listed at the bottom of the table. The speeds VR and V2 are the same for maximum take-off thrust (TOGA). The strong wind speeds of 15 kt headwind and 10 kt tailwind are selected on purpose to magnify the effects on the noise distribution. The runway operating direction is usually in the direction for headwind. Nevertheless, historic flight data include flights operating with similar tailwind speeds. The aircraft departs and flies a straight departure following the waypoints for the entered SID. For simplicity, no climb restriction is considered in this example, although this could also be considered. It should be clearly emphasised that the following results significantly differ between individual take-offs. The results are not transferable to any other take-off case. Their purpose is only the visualisation of the noise reduction potential by individual customised take-off procedures.

#### 3.1 Simulation results

The simulation results of the three exemplary take-offs are compared to a reference departure procedure, and the relative differences are given in percent. The reference procedure is defined to reduce take-off thrust to climb thrust at a height of 1000 ft, then accelerate directly to the final climb speed of 250 kt. The NADP-1 is presented for a thrust reduction height of 800 ft and 1800 ft. By the



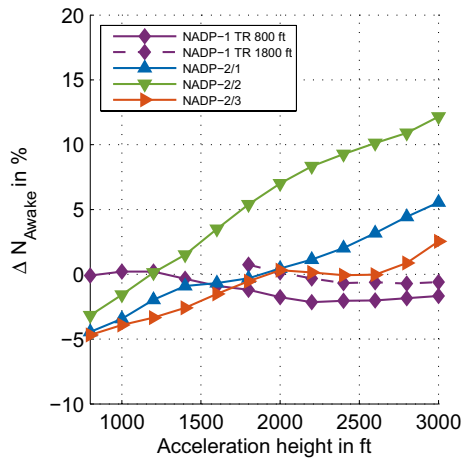


**Fig. 5** Number of awakenings for the noise abatement departure procedures with different acceleration heights as a relative difference to the reference procedure without wind

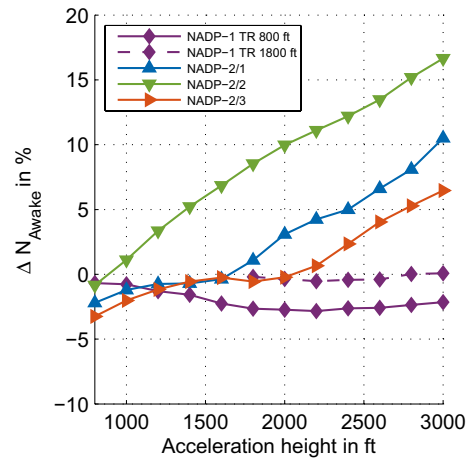


**Fig. 7** Number of awakenings for the noise abatement departure procedures with different acceleration heights as a relative difference to the reference procedure with tailwind

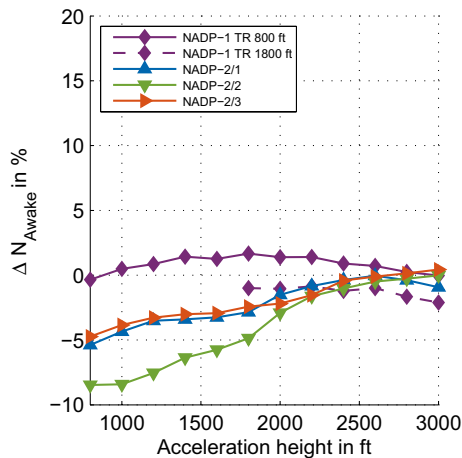


**Fig. 6** Number of awakenings for the noise abatement departure procedures with different acceleration heights as a relative difference to the reference procedure with headwind

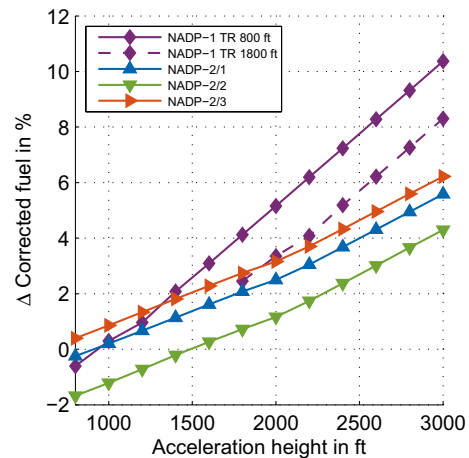


**Fig. 8** Corrected fuel consumption for the noise abatement departure procedures with different acceleration heights as a relative difference to the reference procedure without wind

definition of NADP-1, the procedure is initiated with the thrust reduction. Therefore, the thrust reduction height is equal to the height of the first marker of each line. Each line represents one thrust reduction height and is plotted as a function of the acceleration height. For NADP-2/1, the thrust is reduced with the initiation of flap and slat retraction during the acceleration segment. The NADP-2/2 reduces thrust when the aircraft is clean and NADP-2/3 when the acceleration altitude is reached. The number of awakenings ( $N_{\text{Awake}}$ ) is evaluated for maximum sound pressure levels higher or equal to 60 dB which corresponds to 45 dB for in-door noise levels (partly opened window). This lower limit strongly improves the computational performance, as the grid size can be significantly reduced if a lower noise level limit is defined.

Figures 5, 6, 7 show the number of awakenings as a function of the acceleration height for three considered wind cases. The figures indicate that without wind (Fig. 5) and with tailwind (Fig. 7) NADP-2/3 has the fewest number of awakenings. With headwind (Fig. 6) NADP-2/2 has the fewest number of awakenings. The greatest reduction in the number of awakenings compared to the reference procedure can be achieved with NADP-2/2 in headwind conditions. The number of awakenings can be reduced here by around 8.5 %. The graphs imply that for NADP-2 the number of awakenings increases with the acceleration height. For NADP-1 the number of awakenings tends to increase with the thrust reduction height for the case without wind (Fig. 5) and with tailwind (Fig. 7). With headwind (Fig. 6) the number of awakenings tends to decrease with an increasing

**Fig. 9** Number of people per cell with the drawn contours of the airport and the A-weighted maximum sound pressure levels (70 dB) of NADP-2/2 (acceleration height 800 ft) and the reference procedure with headwind

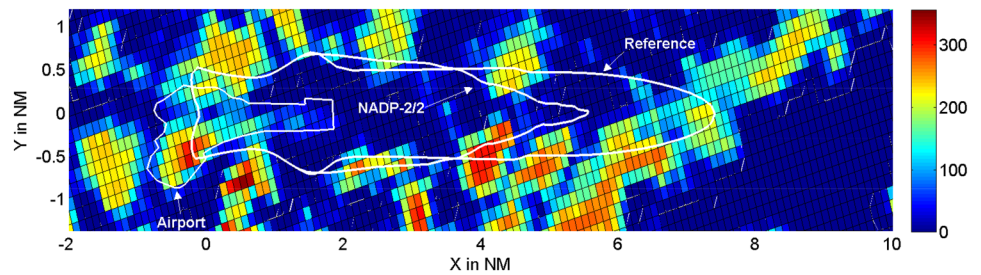
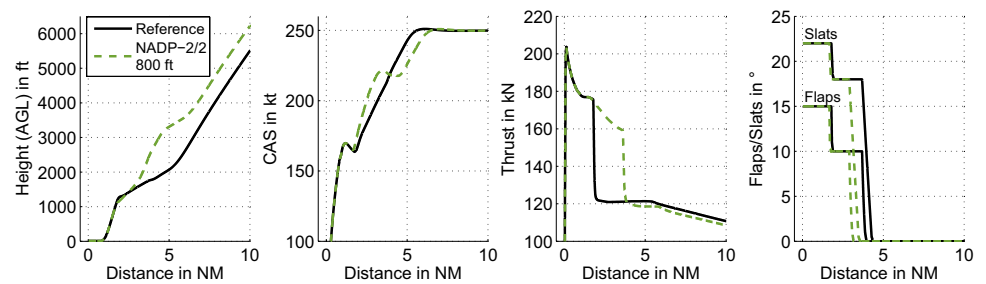


**Fig. 10** Flight parameters for the NADP-2/2 (acceleration height 800 ft) and the reference procedure with headwind



thrust reduction height. Furthermore, for NADP-1 the number of awakenings tends either to increase or decrease with the acceleration height depending on the wind direction. Without wind and with tailwind the number of awakenings initially declines and then slightly rises again. For headwind the number initially rises and then declines.

Figure 8 illustrates the distance-corrected fuel consumption for the case without wind (Fig. 5). The lower the acceleration height, the smaller the aerodynamic drag and the greater the fuel savings. The NADP-2/2 with a thrust reduction when the aircraft is clean indicates the lowest fuel consumption. Flying NADP-2/2 with an acceleration height of 800 ft could reduce fuel consumption by around 1.7 %. The NADP-1 with thrust reduction at 800 ft and an acceleration height of more than 1300 ft indicates the highest fuel consumption. The fuel consumption for a thrust reduction at 1800 ft is lower than for a thrust reduction at 800 ft for the full acceleration height range for which NADP-1 is defined, i.e., 1800 ft and higher. The increase in fuel consumption for an acceleration height of 3000 ft ranges from around 4.3 % (NADP-2/2) to 10.4 % (NADP-1 with thrust reduction at 800 ft).

Figures 9 and 10 visualise the noise reduction between NADP-2/2 with an acceleration height of 800 ft and the reference procedure for headwind conditions (Fig. 6). Figure 9 shows the both contours of a maximum sound pressure level of 70 dB, the population distribution (number of people per cell), and the manually determined airport contour area. The  $x$ -axis is rotated and orientated into the runway direction. Figure 10 shows the corresponding aircraft height above ground level (AGL), calibrated airspeed (CAS), thrust, and the position of flaps and slats over the track distance. It can be seen that the area of the NADP-2/2 noise contour and

the included settlement areas are clearly smaller than of the reference procedure (Fig. 9). The reference procedure reduces thrust at around 1.8 NM which leads to a thinner contour close to the end of the runway. The NADP-2/2 contour remains slightly wider for approximately 2 NM. The same thrust reduction effect can be seen at around 3.6 NM for NADP-2/2. The aircraft gained already more height and the timing for flap retraction and a climb with constant airspeed are very close to each other. Each action reduces noise and affects the contour. Consequently, these effects are slightly overlaid and the appearance is less noticeable than in the reference contour. The slight thinning of the contours at around 3.2 NM (NADP-2/2) and 4.5 NM (Reference) are caused by the retraction of the high-lift devices. Due to the steeper climb with  $V_{zf} + 10$  kt until around 4.5 NM and the following acceleration to 250 kt, the NADP-2/2 contour ends more sudden and sharper. The maximum sound pressure level directly below the aircraft is only higher during the first acceleration segment to  $V_{zf} + 10$  kt starting at a 200 ft lower acceleration height and with maintaining take-off thrust until the aircraft is clean.

### 3.2 Discussion

The results show how different parameters, such as wind, can affect the noise impact, if the take-off procedure is adjusted accordingly. The example visualises that the number of awakenings depends on the selected departure procedure with consideration of the current wind condition. The characteristic of the profiles as shown in Figs. 5, 6, 7 is varying for different parameters (e.g., take-off mass, take-off thrust reduction) and the underlying population distribution resulting from the airport studied, the runway, and the lateral

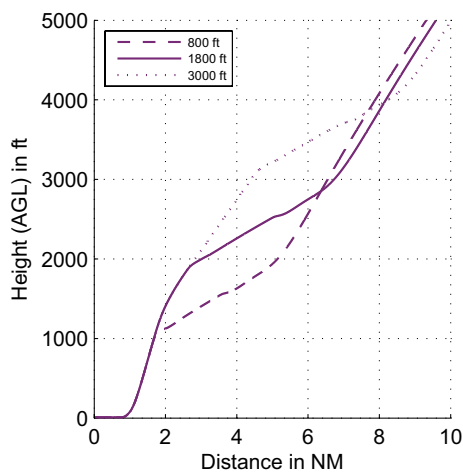


**Fig. 11** Height profiles of the NADP-1 for three different acceleration heights and thrust reduction at 800 ft

routing. This example underlines the noise reduction potential of customising noise abatement departure procedures. Figure 8 indicates that the fuel consumption of NADP-1 tends to be higher than of NADP-2. This behaviour agrees with the reputation of NADP-2 to be more fuel efficient. The example without wind shows that flying a NADP-2/2 can reduce the number of awakenings (Fig. 5). At the same time fuel consumption can be reduced (Fig. 8). As NADP-2/2 maintains take-off thrust until the aircraft is clean, this procedure has the greatest acceleration capability and thus reaches the clean and low drag configuration after the least amount of time. As it uses take-off thrust for the longest time and reaches the low drag configuration first, NADP-2/2 has also the greatest climb capability of NADP-2. Therefore, the aircraft reaches higher altitudes and the top of climb in less time. This might be the reason for the lowest fuel consumption. This performance effect could change for highly reduced take-off thrust. However, flying for a long time with a high thrust level also increases engine stress and might decrease service life and/or increase maintenance cost. Maximum take-off thrust is also limited to a duration of a few minutes. For the population distribution analysed in this study, NADP-1 implies a turning point in the number of awakenings over the acceleration height (Figs. 5, 6, 7). As each curve of NADP-1 starts at the thrust reduction height, the thrust rating for each curve is maximum climb thrust, regardless of the acceleration height. As the thrust rating is equal, the aircraft height and the affected population might be the key reasons for the turning point. A greater height reduces the noise levels on the ground track but can increase the noise to the side of the ground track. For increasing acceleration heights, the height profiles tend to move first to higher heights. Then, after the acceleration segment, the aircraft climbs with constant airspeed

and accordingly with a steeper climb angle. This point is reached first with the lowest acceleration height. This results in higher height profiles for lower acceleration heights more distant from the airport. This characteristic is demonstrated in Fig. 11 with exemplary height profiles for thrust reduction at 800 ft and three different acceleration heights for headwind conditions (Fig. 6). It can be seen that a medium acceleration height of 1800 ft results in the lowest height between around 6.5–8 NM. With increasing tailwind, this segment with the lowest height shifts into the direction of flight. In this example and its population distribution a low populated area begins at around 7.7 NM. The turning points could be induced by these effects and the underlying population distribution.

## 4 Summary and outlook

This paper describes the development of a system which assists pilots during pre-flight planning in order to fly customised low-noise departures. The customisation takes into consideration the individual boundary conditions of a single departure (e.g., wind speed, take-off mass, take-off thrust setting, SID, population distribution). For this reason, the function of this system can be a method and an enabler to replace the previously fix departure procedure definitions for an aircraft type of an operator. It comprises flight simulation, noise computation, and real population data to assess the actual noise impact. A conceptual design is presented and the benefit and the potential of the customisation is demonstrated by examples with initial results. The results demonstrate for the example of three different wind conditions that influencing parameters can individually affect the flight trajectory and therefore the noise on the ground. However, it also becomes apparent that modelling these details requires reliable and accurate simulation tools. The accuracy of the trajectory prediction of the present state of development is susceptible to influencing factors, simplified flight guidance, manual pilot actions, and the models itself (e.g., aerodynamics, thrust, vertical guidance modes). A precise wind prediction is complex. Wind strongly affects the flight performance, the vertical flight trajectory and thus the distance to the ground which affects noise levels on ground. Inaccuracy in lateral flight guidance misrepresents the flight track, which affects the aircraft position and the distance to observers on ground. An online pilot assistance system which is updated with the real wind conditions and aircraft state could be more effective. This would require integration in the automatic flight guidance to follow the updated optimised trajectory. An application in flight operation would also require short flight and noise simulation times. The noise prediction of a single event is subject to significant uncertainties. These uncertainties increase if

wind is present, because wind is not considered in the noise prediction. A different noise prediction method may lead to different results. In the future, it is pursued to use the noise prediction as described in the DIN 45689. As shown in this study, some populated areas can become exposed to higher noise levels if the number of awakenings is the target quantity. This could be resolved if a corresponding boundary condition was added, e.g., an increase of the noise levels in populated areas could be forbidden or at least penalised during the optimisation. Furthermore, a trade-off between noise reduction, fuel consumption, and time might be essential for aircraft operators. For this reason, other evaluation criteria may be applied in the future. Knowledge about prediction uncertainties can also be considered within the evaluation to ensure reliable operational noise recommendations. Population data with a higher resolution might be required for the implementation of such a system into flight operation. Special attention could also be given to areas that are particularly vulnerable (e.g., medical facilities). Further research and development on the conceptual design is ongoing. For this reason, enhancements in the prediction accuracy, the customisation/optimisation, and in the software performance are expected in future. For example, an enhanced live wind model that is based on transmitted wind information from other aircraft might be upcoming. The long-term objective is the integration of the functionality directly into the on-board systems, as in particular the Flight Management and Guidance System (FMGS).

**Funding** Open Access funding enabled and organized by Projekt DEAL. This study was part of the DLR project Fluid-21 (Entwicklung der Fluglärmsituation in Deutschland im 21. Jahrhundert), which was internally funded.

**Data availability** Data of the proposed system is not published/available.

## Declarations

**Conflict of interest** The authors have no competing interests to declare that are relevant to the content of this article.

**Open Access** This article is licensed under a Creative Commons Attribution 4.0 International License, which permits use, sharing, adaptation, distribution and reproduction in any medium or format, as long as you give appropriate credit to the original author(s) and the source, provide a link to the Creative Commons licence, and indicate if changes were made. The images or other third party material in this article are included in the article's Creative Commons licence, unless indicated otherwise in a credit line to the material. If material is not included in the article's Creative Commons licence and your intended use is not permitted by statutory regulation or exceeds the permitted use, you will need to obtain permission directly from the copyright holder. To view a copy of this licence, visit <http://creativecommons.org/licenses/by/4.0/>.

## References

1. European Union Aviation Safety Agency: European aviation environmental : report 2022 (2022). <https://doi.org/10.2822/04357>. URL [https://www.easa.europa.eu/eco/sites/default/files/2022-09/220723\\_EASA%20EAER%202022.pdf](https://www.easa.europa.eu/eco/sites/default/files/2022-09/220723_EASA%20EAER%202022.pdf). Accessed 01.02.2023
2. European Union Aviation Safety Agency: European aviation environmental: report 2019. Publications Office (2019). <https://doi.org/10.2822/309946>. Accessed 11.08.2021
3. World Health Organization: Environmental Noise Guidelines for the European Region. World Health Organization, Regional Office for Europe, Copenhagen, Denmark (2018). [https://www.euro.who.int/\\_\\_data/assets/pdf\\_file/0008/383921/noise-guidelines-eng.pdf](https://www.euro.who.int/__data/assets/pdf_file/0008/383921/noise-guidelines-eng.pdf). Accessed 17.08.2021
4. European Commission: Flightpath 2050: Europe's Vision for Aviation; Maintaining Global Leadership and Serving Society's Needs; Report of the High-Level Group on Aviation Research. Policy / European Commission. Publ. Off. of the Europ. Union, Luxembourg (2011). <https://ec.europa.eu/transport/sites/default/files/modes/air/doc/flightpath2050.pdf>. Accessed 10.08.2021
5. International Civil Aviation Organization: Guidance on the Balanced Approach to Aircraft Noise Management (2008). [http://www.bazl.admin.ch/dam/bazl/de/dokumente/Fachleute/Flugplaetze/ICAO/icao\\_doc\\_9829\\_guidanceonthebalancedapproachtoaircraftnoisemanage.pdf.download.pdf/icao\\_doc\\_9829\\_guidanceonthebalancedapproachtoaircraftnoisemanage.pdf](http://www.bazl.admin.ch/dam/bazl/de/dokumente/Fachleute/Flugplaetze/ICAO/icao_doc_9829_guidanceonthebalancedapproachtoaircraftnoisemanage.pdf.download.pdf/icao_doc_9829_guidanceonthebalancedapproachtoaircraftnoisemanage.pdf). Accessed 20.07.2022
6. Deutsches Zentrum für Luft- und Raumfahrt e.V.: Leiser Flugverkehr: Zusammenfassender Projekt-Abschlussbericht (2004). [https://www.dlr.de/as/Portaldata/5/Resources/dokumente/abteilungen/abt\\_ts/Abschlussbericht\\_LFVK.pdf](https://www.dlr.de/as/Portaldata/5/Resources/dokumente/abteilungen/abt_ts/Abschlussbericht_LFVK.pdf). Accessed 20.07.2022
7. European Commission: Commission Regulation (EC) No 859/2008 of 20 August 2008 amending Council Regulation (EEC) No 3922/91 as regards common technical requirements and administrative procedures applicable to commercial transportation by aeroplane (2008). <https://eur-lex.europa.eu/legal-content/EN/ALL/?uri=celex:32008R0859>. Accessed 28.04.2022
8. International Civil Aviation Organization: Procedures for Air Navigation Services - Aircraft Operations. Volume I - Flight Procedures: Doc 8168 (2006). [http://www.chcheli.com/sites/default/files/icao\\_doc\\_8168\\_vol\\_1.pdf](http://www.chcheli.com/sites/default/files/icao_doc_8168_vol_1.pdf). Accessed 20.07.2022
9. Roman-Georg Huemer: Entwicklung von lärmindernden operationell einsetzbaren Abflugverfahren (2004). <https://elib.dlr.de/5811/>. Accessed 20.07.2022
10. Kühne, C. G., Scholz, M., Abdelmoula, F.: LNAS – A Pilot Assistance System for Energy-Optimal Approaches Using Existing Aircraft-Infrastructure, Toulouse, France (2018). <https://elib.dlr.de/122571/>. Accessed 20.07.2022
11. Maoui, G.: Innovation Takes Off : Clean Sky : European Research for Aeronautics. Le cherche midi éditeur, Paris (2016)
12. Albert, M., Cadot-Burillet, D., Williams, A.: Integration of Mission Trajectory Management Functions Into Clean Sky Technology Evaluation Process (2015). [https://aerospace-europe.eu/media/books/CEAS2015\\_100.pdf](https://aerospace-europe.eu/media/books/CEAS2015_100.pdf). Accessed 19.06.2023
13. Airbus: A320 Flight Crew Operating Manual: Vol. 1: Systems Description (Issue Date 01.12.2008)
14. Airbus: A320 Flight Crew Operating Manual: Vol. 2: Flight Preparation (Issue Date 01.09.2009)
15. Airbus: A320 Flight Crew Operating Manual: Vol. 3: Flight Operations (Issue Date 01.06.2009)
16. Airbus: A320 Flight Crew Operating Manual: Vol. 4: FMGS Pilot's Guide (Issue Date 01.03.2009)
17. Airbus Industrie: A320 Flight Manual: Model 320-232, Blagnac, France (Issue Date 13.10.2008)

18. Airbus S. A. S.: A320/A321 Aircraft Maintenance Manual AMM: Aero Lloyd, Blagnac Cedex, France (Revision Date 01.05.2009)
19. Schaffarczyk, A. (ed.): Einführung in die Windenergietechnik: Mit 27 Tabellen Sowie Zahlreichen Beispielen und Übungen. Fachbuchverl. Leipzig im Carl-Hanser-Verl, München (2012)
20. European Civil Aviation Conference: ECAC.CEAC Doc 29 - Report on Standard Method of Computing Noise Contours around Civil Airports: Volume 1: Applications Guide: 4th Edition (2016)
21. European Civil Aviation Conference: ECAC.CEAC Doc 29 - Report on Standard Method of Computing Noise Contours around Civil Airports: Volume 2: Technical Guide: 4th Edition (2016)
22. European Civil Aviation Conference: ECAC.CEAC Doc 29 - Report on Standard Method of Computing Noise Contours around Civil Airports: Volume 3, Part 1 - Reference Cases and Verification Framework: 4th Edition (2016)
23. AzB - Anleitung zur Berechnung von Lärmschutzbereichen: Vom 19. November 2008. In: Bundesanzeiger vol. 195a vom 23.12.2008
24. Ulrich Isermann: Berechnung der Fluglärmimmission in der Umgebung von Verkehrsflughäfen mit Hilfe eines Simulationsverfahrens. Dissertation, Max-Planck-Institut für Strömungsforschung, Göttingen (1988)
25. Isermann, U., Binder, U., Boguhn, O., Schmid, R.: DLR-Projekt Leiser Flugverkehr II, Abschlussbericht zum Hauptarbeitspaket Fluglärmprognose (2008). <https://elib.dlr.de/57018/>
26. Schiavina, M., Freire, S., MacManus, K.: GHS population grid multitemporal (1975-1990-2000-2015), R2019A. European Commission, Joint Research Centre (JRC). <https://doi.org/10.2905/0C6B9751-A71F-4062-830B-43C9F432370F>
27. European Commission, Joint Research Centre, Ehrlich, D., Florczyk, A., Pesaresi, M., Maffellini, L., Schiavina, M., Zanchetta, L., Politis, P., Kemper, T., Sabo, F., Freire, S., Corbane, C., Melchiorri, M.: GHSL data package 2019 : public release GHS P2019. Publications Office (2019). <https://doi.org/10.2760/062975>
28. Basner, M., Samel, A., Isermann, U.: Aircraft noise effects on sleep: Application of the results of a large polysomnographic field study. *J. Acoust. Soc. Am.* **119**(5, Pt 1 of 2), 2772–2784 (2006). <https://doi.org/10.1121/1.2184247>

**Publisher's Note** Springer Nature remains neutral with regard to jurisdictional claims in published maps and institutional affiliations.